Downloaded from UvA-DARE, the institutional repository of the University of Amsterdam (UvA)
http://hdl.handle.net/11245/2.2527

File ID	uvapub:2527
Filename	2300857.pdf
Version	unknown

SOURCE (OR PART OF THE FOLLOWING SOURCE):

Type	article
Title	Energy dependence in the QPO and noise of black-hole candidates in the very high state
Author(s)	T. Belloni, M. van der Klis, W.H.G. Lewin, J.A. van Paradijs, T. Dotani, K. Mitsuda, S. Miyamoto
Faculty	FNWI: Astronomical Institute Anton Pannekoek (IAP)
Year	1997

FULL BIBLIOGRAPHIC DETAILS:
http://hdl.handle.net/11245/1.132620

Copyright

It is not permitted to download or to forward/distribute the text or part of it without the consent of the author(s) and/or copyright holder(s), other than for strictly personal, individual use, unless the work is under an open content licence (like Creative Commons).

UvA-DARE is a service provided by the library of the University of Amsterdam (http://dare.uva.nl)
(pagedate: 2014-11-14)

Astron. Astrophys. 322, 857–867 (1997)

ASTRONOMY AND ASTROPHYSICS

Energy dependence in the quasi-periodic oscillations and noise of black hole candidates in the very high state

T. Belloni[1], M. van der Klis[1], W.H.G. Lewin[2], J. van Paradijs[1,3], T. Dotani[4], K. Mitsuda[4], and S. Miyamoto[5]

[1]Astronomical Institute "Anton Pannekoek", University of Amsterdam and Center for High-Energy Astrophysics, Kruislaan 403, 1098 SJ Amsterdam, The Netherlands

[2]Massachusetts Institute of Technology, Center for Space Research, Room 37-627, Cambridge, MA 02139, USA

[3]Physics Department, University of Alabama in Huntsville, AL 35899, USA

[4]Institute of Space and Astronautical Science, 3-1-1, Yoshinodai, Sagamihara, Kanagawa 229, Tokyo, Japan

[5]Osaka University of Health and Sport Science, Noda 1558-1, Kumatori-cho, Sennan-gun, Osaka, 590-04, Japan

Received 28 May 1996 / Accepted 10 December 1996

Abstract. We present the results of an energy-dependent timing analysis of Ginga data from the black hole candidates GS 1124-68 and GX 339-4 in their Very High State (VHS). Large variations with energy of the timing properties are seen in both sources. The break frequency of the band-limited noise increases with energy, indicating considerable spectral changes on sub-second timescales. Quasi-periodic oscillations (QPOs) with high (and energy dependent) harmonic content are observed, whose peaks in the power spectra appear to be asymmetric. The fractional amplitude of the fundamental QPO peak increases with energy and the QPO harmonic content *decreases* with energy, indicating that the at higher energies the QPO cycle becomes more sinusoidal. During one observation of GS 1124-68, the QPO centroid frequency increases with decreasing 9-30 keV source count-rate. We found a previously unknown 6.7 Hz QPO peak, also energy dependent, in GS 1124-68, four months after the peak of the outburst. The energy dependence of the band-limited noise is interpreted in the frame of a shot-noise model with softening shots. The complex phenomenology reported here puts strong constraints on the theoretical models for spectral distribution and time variability of black hole candidates at high accretion rates.

Key words: X-rays: stars – stars: individual, GS 1124-68, GX 339-4 – binaries: close

1. Introduction

During the first half of this decade the known phenomenology of aperiodic time variability in Black Hole Candidates has considerably increased in complexity (see Van der Klis 1995 for a review). The data from the Ginga satellite have allowed detailed studies of the transient sources belonging to this category. In particular, besides the 'high' and 'low' states (first identified in Cyg X-1 by Tananbaum et al. 1972 on the basis of the X-ray spectral distribution), a third state has been recognized, corresponding to high luminosities, probably connected to near-Eddington accretion rates (Miyamoto et al. 1991). This state is characterized by a two-component X-ray spectrum, consisting of a strong thermal spectrum which dominates the flux below a few keV, and a hard power law extending to higher energies (see Miyamoto et al. 1991, Ebisawa et al. 1994). The temporal variability is characterized by the presence of a 3-10 Hz QPO peak with complex harmonic content, plus either a band-limited noise or a weaker power law noise component (Miyamoto et al. 1994a, Takizawa et al. 1996). This very-high state (VHS) has been observed with Ginga in only two sources so far, the transient GS 1124-68 (Ebisawa et al. 1994, Miyamoto et al. 1994a) and during a single observation of the persistent system GX 399-4 (Miyamoto et al. 1991).

In this paper we present results of an analysis of the energy dependence of the QPO and noise components in the power spectra of these two sources, as observed with Ginga.

2. Data analysis

We analyzed data of GS 1124-68 and GX 339-4 from the LAC on board Ginga (Turner et al. 1989). All data are from observing mode MPC3, with a time resolution of 7.8 ms and 12 energy channels covering the range 1.2-37.0 keV. For GS 1124-68, we selected three observations early in its outburst in January 1991, and a later observation in May 1991. During this observation the source was in a transition between high and low state (see Ebisawa et al. 1994), and its timing characteristics are surprisingly similar to those in the VHS, although at a much lower X-ray luminosity (Miyamoto et al. 1994a). For GX 339-4 we consid-

Send offprint requests to: T. Belloni

ered the only observation of the source in the VHS (September 1988, see Miyamoto et al. 1991). Given the high variability in the source properties (Miyamoto et al. 1991), this observation was subdivided into two parts. A log of the observations is reported in Table 1. The high-energy channels have been combined and the lowest channel has not been used so that a total of four energy bands were considered, with the exception of the May 17 observation of GS 1124-68 where further rebinning was applied (see Table 1).

3. Power density spectra

For each observation and each separate energy band, power spectra have been produced from short stretches of data. These were averaged together and rebinned in energy when necessary to increase the source signal. The power density spectra have been normalized to squared fractional rms according to Belloni and Hasinger (1990b) by using the total and background count rates. A logarithmic rebinning in frequency has been applied to the power spectra. The white-noise level due to Poissonian statistics as modified by dead-time effects was subtracted.

We fitted the resulting power spectra to analytic models using a χ^2 minimization technique to obtain values of the fit parameters as a function of energy.

For the visual presentation of the data, we plot the power spectra not as fractional rms^2/Hz vs. frequency ν, but as fractional rms^2 $\times$ ν/Hz vs. ν. This convention has a number of advantages. Since the quantity plotted is now rms$^2/d(\log\nu)$, a logarithmic plot gives a direct visual idea of the rms distribution. Moreover, Lorentzian functions as used in our model (see below) now become symmetric in log-log plots. They have a maximum at a frequency

$$\nu_{max} = \sqrt{\nu_0^2 + (\frac{\Delta}{2})^2} \quad (1)$$

where ν_0 is the central frequency and Δ is the FWHM of the Lorentzian. This means that a Lorentzian band-limited noise (ν_0=0) has a maximum at a frequency equal to its break frequency (defined as $\nu_{\rm BLN} = \Delta_{\rm BLN}/2$), making it easier to see changes in the latter. A disadvantage is that a Lorentzian QPO has its maximum at a frequency higher than its central frequency, but for the power spectra shown in this paper this turns out to be a small effect. We remark that this new convention has been followed *only* for producing the plots, while all analytic fits (see below) have been performed directly on the original power spectra. An example illustrating the two different representations is shown in Fig. 1, where a model consisting of a band-limited noise plus a QPO peak, both Lorentzians in shape, is plotted.

4. Results

4.1. The analytic model

The first column of plots in Fig. 2 shows two of the the power spectra of the Jan-11 observation of GS 1124-68, the one with the largest contribution from the hard spectral component; it is clear that no simple model would be able to represent the data. Although the shape of the band-limited noise is relatively simple, the high (and variable) harmonic content of the QPO requires a considerable number of parameters. Moreover, the shape of the QPO peaks is asymmetric, suggesting the use of a more complex model than a simple Lorentzian function. The most characteristic part of the band-limited noise (i.e. the break) appears in the same range of frequencies as the QPO peaks. Therefore, in order to obtain reliable parameters it is necessary that the quality of the fits is good, and therefore the model must use a considerable number of free parameters. To extract meaningful information from the data, the same model should be applied to all the power spectra. This means that all the features of all spectra should be included: a large number of asymmetrical QPO peaks and a band-limited noise component. In the 7.0-9.3 keV spectrum of Jan 11 (Fig. 2, top panel) four QPO peaks can be seen: identifying the strongest one with the fundamental frequency (see below), these peaks correspond to sub-harmonic, first, second and fourth harmonic. Since an estimate of the possible presence of a weak third harmonic would be needed, a fifth peak should be added. By adopting lorentzian shapes for the band-limited noise and the QPO peaks, a total of 18 parameters would be needed. More parameters would come from additional components introduced in order to account for the asymmetry of the QPO peaks. Many of those free parameters would not be constrained for some components in some power spectra, resulting in unreasonable best fit values. We adopted a model which, despite its relatively high number of free parameters, does not suffer of these problems and can be used for all the power spectra from our data. This model is entirely based on the power spectra of Jan 11, where the quality is high and the largest number of QPO peaks is visible.

The model consists of a lorentzian band-limited noise, plus up to five lorentzian QPO peaks, each with a second lorentzian ("shoulder") to account for the peak asymmetry. In order to reduce the number of free parameters, the following additional constraints have been added:

– The central frequencies of the QPO peaks have been fixed to harmonic ratios. Simple fits with lorentzian shapes to the four peaks in the power spectrum from the 7.0-9.3 keV range show that the frequency peaks are harmonically related. Fol-

Table 1. Observation log. Column 5 contains the number of energy bands considered; channel ranges are 2,3,4,5-12 for the four-band cases and 2,3-12 for the 2-band case. Numbers in column 6 are uncorrected MPC3 count rates.

Date	UT Start	UT End	Exp. (s)	# B	Rate (c/s)
		GS 1124-68			
91 Jan 11	20:53	23:59	6656	4	13571
91 Jan 22	17:21	19:41	8192	4	15776
91 Jan 25	11:59	18:56	2560	4	13433
91 May 17	06:06	06:53	3712	2	1433
		GX 339-4			
88 Sep 5 (C)	14:58	17:04	5696	4	4546
88 Sep 5 (D)	13:24	13:53	2816	4	4033

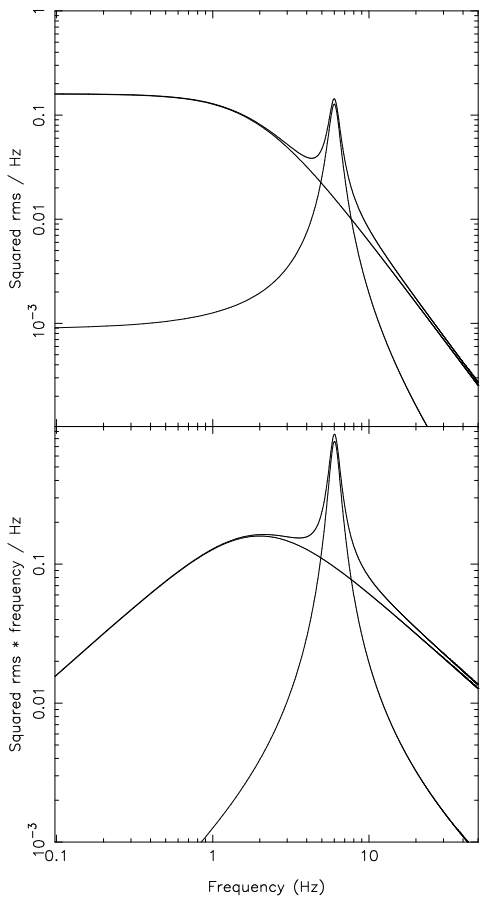

Fig. 1. Model power spectrum consisting of the sum of two Lorentzian functions: a band-limited noise component ($\nu_0 = 0, \nu_{BLN} = 2.0$ Hz) and a QPO peak ($\nu_0 = 6.0, \Delta = 1.0$ Hz. The top panel shows a conventional $P(\nu)$ vs. ν view of the power spectrum, the bottom panel shows $\nu \times P(\nu)$ vs. ν (see text).

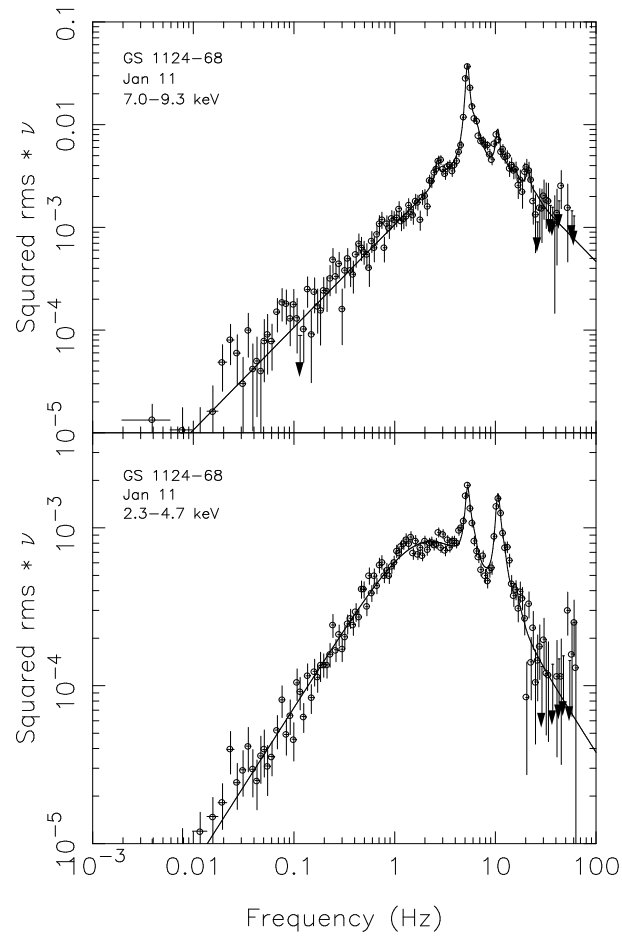

Fig. 2. Two power spectra of the 1991 Jan 11 observation of GS 1124-68. The best fits obtained with the model described in the text are shown.

lowing Takizawa et al. (1996) we considered as *fundamental* or *first harmonic* the peak with the largest fractional rms in the hard energy band, as second, third and fourth harmonics the peaks at higher frequencies, and as sub-harmonic the one at half the frequency of the fundamental.

– The FWHM of the QPO peaks have also been fixed to harmonic ratios. This is derived from the 2.3-4.7 keV and 4.7-7.0 keV power spectra of Jan 11, the only two spectra where two strong peaks are observed. Lorentzian fits to those peaks yielded values of the FWHMs supporting this hypothesis. It is clear that the extension of this result to higher harmonics and to other observations is an extrapolation.
– The shape of the asymmetry in the QPO peaks has been fixed to be the same for each observation. This has been achieved by harmonically relating the central frequencies and FWHMs of the "shoulder" lorentzians, and by tying their normalization to be the same percentage of the normalization of the corresponding QPO lorentzian. Once again, this is a result based on the two strong peaks in the 2.3-4.7 keV and 4.7-7.0 keV power spectra of Jan 11.

This model provides a reasonable fit to the data, but still the fits are not perfect: releasing some of the above constraints, we found that the unconstrained components would try to fit other parts of the power spectra.

The model has 17 free parameters, many of which are normalizations. It has to be stressed that for single power spectra this might not be the best model in terms of chi square, but it provides a global homogeneous interpretation of the power spectra of black hole candidates in the VHS. Two examples of fits with the adopted model from the GS 1124-68 Jan 11 data are shown in Fig. 2.

In summary, the adopted model consists of a band-limited noise component (BLN), a multi-harmonic QPO component and a shoulder component (SHL) to represent the high-frequency wing of the QPO peaks:

$$P(\nu) = BLN(\nu) + QPO(\nu) + SHL(\nu) \quad (2)$$

The three separate components have the following form:

$$BLN(\nu) = L(\nu; R_{BLN}, 0, 2 \cdot \nu_{BLN}) \quad (3)$$

$$QPO(\nu) = L\ (\nu; R_{QPO_{1/2}}, \frac{1}{2}\nu_{QPO}, \frac{1}{2}\Delta_{QPO}) + \sum_{j=1}^{4} L(\nu; R_{QPO_j}, j \cdot \nu_{QPO}, j \cdot \Delta_{QPO}) \quad (4)$$

$$SHL(\nu) = L\ (\nu; f \cdot R_{QPO_{1/2}}, \frac{1}{2}\nu_{SHL}, \frac{1}{2}\Delta_{SHL}) + \sum_{j=1}^{4} L(\nu; f \cdot R_{QPO_j}, j \cdot \nu_{SHL}, j \cdot \Delta_{SHL}) \quad (5)$$

where $L(\nu; R, \nu_0, \Delta)$ is a Lorenztian function with integral R, central frequency ν_0 and FWHM Δ

$$L(\nu; R, \nu_0, \Delta) = \frac{R\Delta}{2\pi} \frac{1}{(\nu - \nu_0)^2 + (\frac{\Delta}{2})^2} \quad (6)$$

The relevant parameters of the model are:

ν_{BLN} break frequency of the noise component.
ν_{QPO} frequency of the fundamental tone of the QPO.
Δ_{QPO} FWHM of the fundamental tone of the QPO.
ν_{SHL} central frequency of the fundamental tone of the "shoulder" of the QPO.
Δ_{SHL} FWHM of the fundamental tone of the "shoulder".

The remaining parameters are the normalizations of the noise and of the harmonic peaks (the R's), and the amplitude of the shoulder relative to the QPO peak, f. The latter is the same for all harmonics. Although the model appears rather complex, involving a large number of free parameters, it puts rather strong constraints on the fit by having only 5 free parameters in addition to the up to 7 normalization parameters. Not for all observations all the components have been included, and depending on the shape of the spectra and their statistical significance, some of the parameters have been frozen for some fits. In particular, the shoulder component has been included only for the Jan 11 and Jan 22 spectra of GS 1124-68, and only in the case of Jan 11 all five harmonic peaks have been used. Moreover, when the power distribution showed evidence of an additional steep component at very low frequencies (see Miyamoto et al. 1994a), the lowest frequency points have been removed before the fits, while the rest of the power spectrum is unaffected by it.

The identification of the fundamental described above is of course not unique. In particular, it leaves open the question of the nature of the subharmonic peak, which represents oscillations at twice the period of the fundamental. However, if this lowest frequency peak is identified with the fundamental, the observed peaks would all be even harmonics, which would be as intriguing as the presence of a subharmonic. Moreover, in this scenario the fundamental would not be present at low energies.

For the presentation of the data, the energy dependences of a selected number of parameters are shown in Fig. 4 and 5. These parameters are reported in Table 2. All parameters which do not appear in the plots can be found in Table 3.

4.2. GS 1124-68

Three of the observations considered in the analysis (see Table 1) correspond to times early in the outburst. These are the only data in high time-resolution mode where QPO peaks have been reported (Takizawa et al. 1996). The fourth is a later observation when the source was in its transition to a low (hard) state (Ebisawa et a. 1994). The best fit parameters for the different datasets can be seen in Table 2. The Jan 25 observation does not show any band-limited noise (see Miyamoto et al. 1994a).

4.2.1. Jan 11

This is the observation with the highest-quality power spectra. Although the total count-rate is not higher than in the Jan 22 observation (see Table 1), the energy spectra show that the hard power law component, which has been reported to be the one responsible for the strong noise components (Miyamoto et al. 1994a), is strong. The power spectra in five different energy bands are shown in Fig. 3 (first column). Remarkable differences can be seen between noise components at different energies. The break frequency of the band-limited noise $\nu_{\rm BLN}$ strongly increases with energy, from $\sim$2.2 Hz in the first band (2.3-4.7 keV) to $\sim$10 Hz in the last band (9.3-37.2 keV). The same tendency was observed in Cyg X-1 in its low state (Miyamoto and Kitamoto 1989). The strength of the fundamental QPO peak (at $\sim$ 5.3 Hz) and its sub-harmonic (at $\sim$ 2.6 Hz) also strongly increases with energy. Higher harmonics are present, which are highly variable and sometimes confused in the continuum. In the 7.0-9.3 Hz band *four* clear QPO peaks are visible in the power spectrum, a unique feature in power spectra of accreting X-ray sources. The fundamental peak is clearly asymmetric, justifying the inclusion of a "shoulder" component. The total fractional rms in the shoulder is rather high, between $\sim$50 and $\sim$90 % of the one in the central QPO component. Its FWHM is larger than that of the QPO, and its central frequency less than one hertz higher (see Table 3). The dependence of relevant parameters on energy in shown in Fig. 4 (first column); the remaining parameters (QPO central frequency and FWHM) are compatible with a constant value. It is remarkable that the break frequency of the noise (ν_{BLN}) is lower than ν_{QPO} (which is constant at 5.3 Hz, see Table 3) at low energies, but higher in the last energy bins. This has the effect to increase the level of the band-limited noise at high frequencies, so that the peaks of the higher harmonics are less visible in the higher energy power spectrum.

4.2.2. Jan 22

The power spectra from this observation (second column in Fig. 3) clearly show a behaviour similar to the Jan 11 case. The QPO intensity is strongly energy-dependent and so seems the noise. However, it is clear that the QPO peaks are much broader, and the harmonic content is not as high. From the model fits described above it emerges that the noise break frequency $\nu_{\rm BLN}$ is not monotonically increasing, contrary to what happened 11 days earlier. The shoulder is weaker relative to the QPO, only slightly

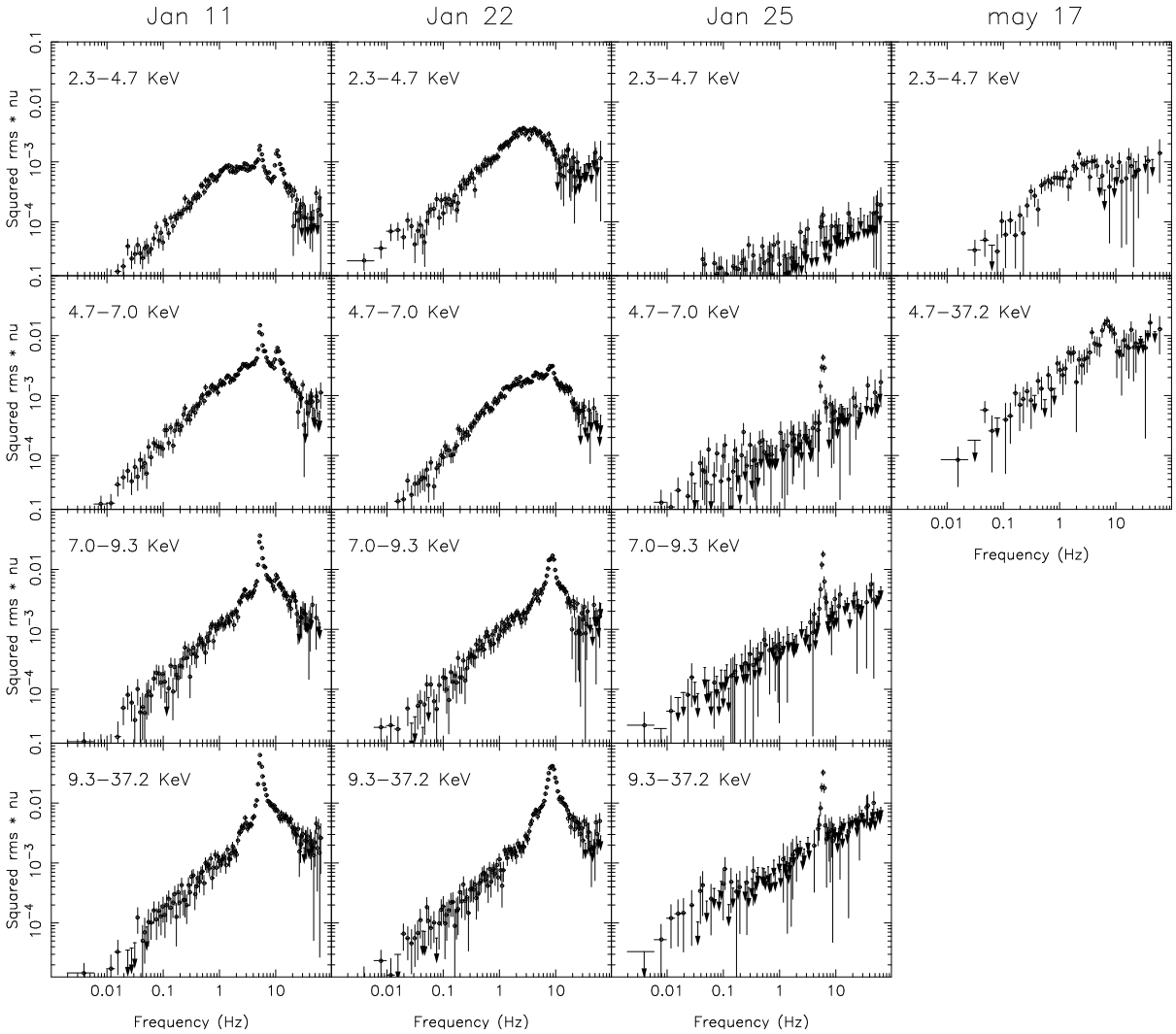

Fig. 3. Power spectra of GS 1124-68 for all the observations described in the text. The energy bands are indicated. The power spectra are plotted as νP_ν, following the representation described in Sect. 3. Data points consistent with null power have been plotted as 2σ upper limits (arrows) for clarity, although the actual values have been used for the fits.

broader, and its frequency considerably higher (see Table 3). For some of the spectra, not all the parameters have been fitted, and for the first two (where the QPO peak is weak) the shoulder parameters have been fixed to the best fit parameters for the high energy power spectra. The results of the fits are shown in Fig. 4 (second column), Again, the parameters not shown in the plot are not observed to show variations with energy.

4.2.3. Jan 25

As already noticed in Miyamoto et al. (1994a), this observation, just three days after the previous one, shows no band-limited noise, although a strong QPO peak is present. This can be seen in Fig. 3, where most of the data consist of upper limits. From Fig. 3 it is evident how the intensity of this QPO peak is also strongly energy-dependent, as in the two previous cases. The QPO rms as a function of energy is shown in Fig. 4 (third column). The model used in this case consists of a single Lorentzian QPO peak plus a band-limited component whose break frequency has been fixed to the best fit values for the Jan 11 observation. This band-limited noise component has been included for comparison with the other observations and its normalization is not significant (see Table 2).

4.2.4. May 17

This observation was performed more than four months after the outburst. The previous pointing (Apr 19) shows the source in the high state, the following (Jun 13) in the low state (Ebisawa et al. 1994). The spectral distribution shows for the high energy tail a photon index $\Gamma \sim 2.2$, intermediate between the ones in the very high (2.6) and low states (1.6), although the photon index is $\sim$2.2 on Jan 10 and at the beginning of Jan 11. (Ebisawa et al. 1994; there is no hard tail in high state). As reported in Miyamoto

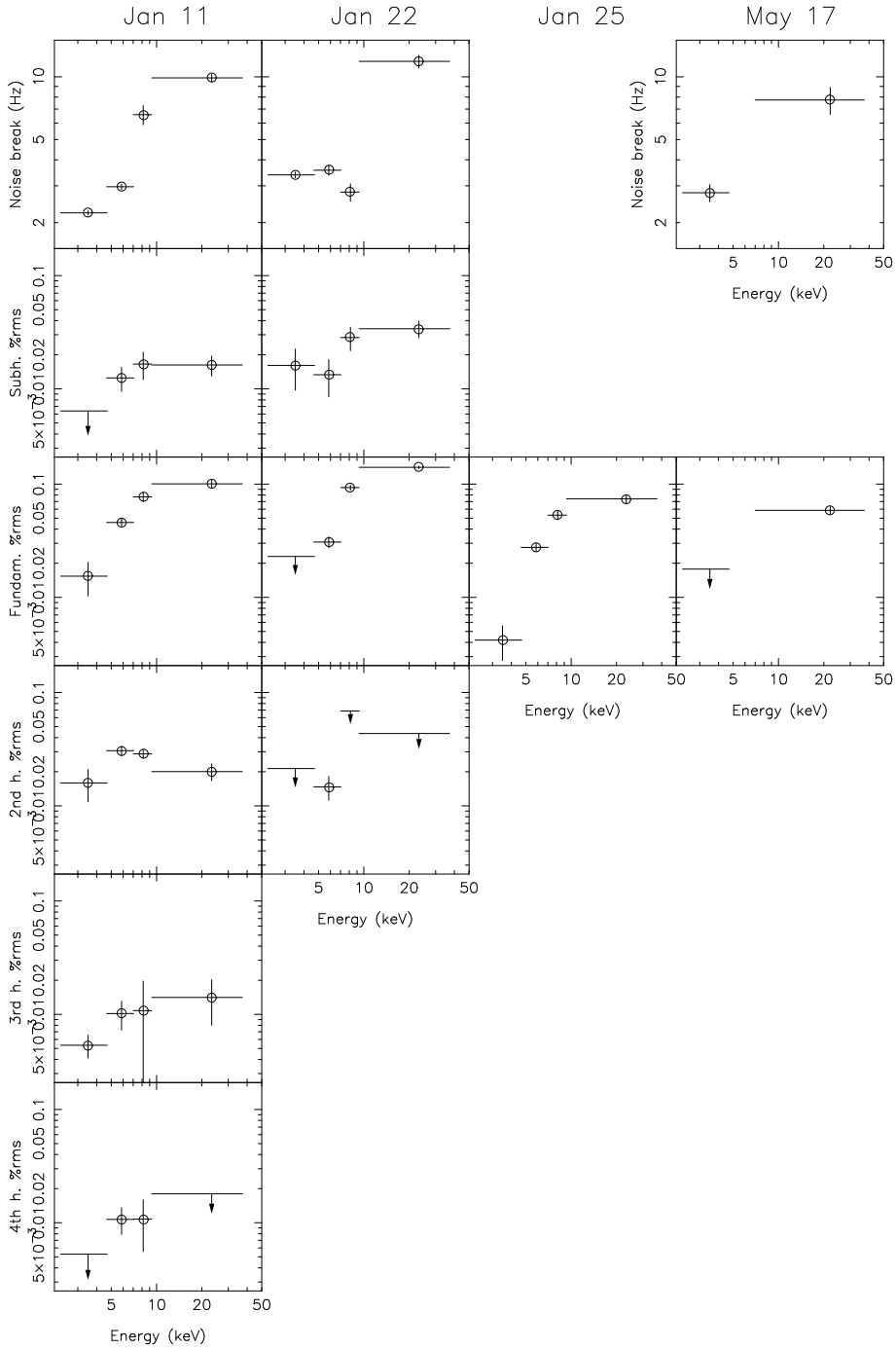

Fig. 4. Energy dependence of selected fit parameters for the observations of GS 1124-68 (see Fig. 3).

et al. (1994a), the power spectrum shows a band-limited noise component similar to that of the VHS. Since the count-rate is significantly lower than in the January observations, we could only produce power spectra in two energy bands, as the high-energy bins had to be further rebinned. The results are shown in Fig. 3 (fourth column). Although the statistics is not very good (and the presence of a break in the power is not clearly visible by eye, due to the presence of several upper limits and to the νP_ν representation), a QPO peak is clearly visible in the power spectrum from the high energy band. Since it is only visible in the high energy data, it was not detected previously (see Miyamoto et al. 1994a, Takizawa et al. 1996). As it can be seen from Fig. 4 and Table 3, its fractional rms and width are not different from those detected in the other observations. Its central frequency of $\sim$ 6.7 Hz does not fit any of the period-intensity relations reported by Takizawa et al. (1996), as the observation was made four months after the peak of the outburst and the source count-rate was considerably lower (see Table 1).

Table 2. Best-fit values for selected parameters for both sources. The energy dependence of the same parameters is shown in Fig. 3. Errors are 1σ, upper limits are 2σ.

Energy (keV)	ν_{BLN} (Hz)	$R_{QPO_{1/2}}$(%)	R_{QPO_1} (%)	R_{QPO_2} (%)	R_{QPO_3} (%)	R_{QPO_4} (%)
GS 1124–68 – 1991 Jan 11						
3.50 ±1.20	$2.23^{+0.06}_{-0.05}$	< 0.64	$(1.54^{+0.28}_{-0.50})$	$(1.59^{+0.33}_{-0.50})$	$(0.53^{+0.15}_{-0.12})$	< 0.53
5.85 ±1.15	$2.97^{+0.25}_{-0.09}$	$(1.25^{+0.37}_{-0.30})$	$(4.58^{+0.47}_{-0.42})$	$(3.01^{+0.19}_{-0.29})$	$(1.01^{+0.32}_{-0.29})$	$(1.07^{+0.31}_{-0.28})$
8.15 ±1.15	$6.59^{+0.53}_{-0.70}$	$(1.66^{+0.28}_{-0.45})$	$(7.70^{+0.64}_{-0.72})$	$(2.87^{+0.40}_{-0.24})$	$(1.08^{+0.84}_{-0.89})$	$(1.08^{+0.67}_{-0.52})$
23.25±13.95	$9.88^{+0.36}_{-0.39}$	$(1.62^{+0.30}_{-0.33})$	$(10.0^{+0.70}_{-0.80})$	$(2.00^{+0.41}_{-0.34})$	$(1.41^{+0.62}_{-0.61})$	< 1.80
GS 1124–68 – 1991 Jan 22						
3.50 ±1.20	$3.39^{+0.11}_{-0.11}$	$(1.61^{+0.64}_{-0.64})$	< 2.30	< 2.14	—	—
5.85 ±1.15	$2.93^{+0.16}_{-0.20}$	$(1.33^{+0.64}_{-0.48})$	$(3.08^{+0.42}_{-0.34})$	$(1.47^{+0.39}_{-0.35})$	—	—
8.15 ±1.15	$4.08^{+0.49}_{-0.27}$	$(2.84^{+0.54}_{-0.56})$	$(9.32^{+0.30}_{-0.51})$	< 6.88	—	—
23.25±13.95	$11.87^{+0.90}_{-0.84}$	$(3.39^{+0.54}_{-0.56})$	$(14.0^{+0.40}_{-0.40})$	< 4.36	—	—
GS 1124–68 – 1991 Jan 25						
3.50 ±1.20	2.23 (FIX)	—	$(0.42^{+0.14}_{-0.14})$	—	—	—
5.85 ±1.15	2.97 (FIX)	—	$(2.76^{+0.23}_{-0.23})$	—	—	—
8.15 ±1.15	6.59 (FIX)	—	$(5.31^{+0.48}_{-0.48})$	—	—	—
23.25±13.95	9.88 (FIX)	—	$(7.40^{+0.61}_{-0.61})$	—	—	—
GS 1124–68 – 1991 May 17						
3.50 ±1.20	$2.78^{+0.29}_{-0.27}$	—	< 1.78	—	—	—
22.1 ± 15.1	$7.75^{+1.11}_{-1.14}$	—	$(5.86^{+0.51}_{-0.44})$	—	—	—
GX 339–4 – Observ. C						
3.50 ±1.20	$1.86^{+0.08}_{-0.07}$	$(1.63^{+0.48}_{-0.49})$	$(1.89^{+0.31}_{-0.33})$	$(1.00^{+0.50}_{-0.53})$	—	—
5.85 ±1.15	$1.73^{+0.10}_{-0.09}$	$(3.44^{+0.75}_{-0.79})$	$(7.43^{+0.45}_{-0.47})$	$(3.15^{+0.66}_{-0.68})$	—	—
8.15 ±1.15	$1.82^{+0.19}_{-0.22}$	$(3.16^{+1.74}_{-1.81})$	$(13.4^{+0.70}_{-0.70})$	$(4.83^{+1.39}_{-1.41})$	—	—
23.25±13.95	$3.30^{+0.80}_{-1.34}$	< 6.30	$(16.9^{+1.20}_{-1.40})$	$(6.22^{+1.86}_{-1.78})$	—	—
GX 339–4 – Observ. D						
3.50 ±1.20	$1.74^{+0.09}_{-0.11}$	$(1.28^{+0.66}_{-0.77})$	$(2.68^{+0.43}_{-0.45})$	$(1.70^{+0.43}_{-0.45})$	—	—
5.85 ±1.15	$1.52^{+0.12}_{-0.10}$	$(4.40^{+0.69}_{-0.84})$	$(8.41^{+0.46}_{-0.56})$	$(4.42^{+0.59}_{-0.66})$	—	—
8.15 ±1.15	$4.62^{+0.86}_{-0.61}$	< 4.26	$(10.6^{+1.10}_{-1.40})$	< 5.46	—	—
23.25±13.95	$9.01^{+1.85}_{-1.88}$	$(3.35^{+1.68}_{-1.73})$	$(13.9^{+1.10}_{-1.10})$	$(3.42^{+3.01}_{-3.24})$	—	—

4.3. GX 339-4

As mentioned above, the observation has been divided into two parts, corresponding to states C and D of this source in Miyamoto et al. (1991). The power spectra can be seen in Fig. 5. Although their quality is not as high as for those of GS 1124-68, especially at high frequencies, there is a remarkable similarity between the two sets of power spectra. The break frequency ν_b and the rms of the fundamental QPO peak increase with energy and higher harmonics become less visible at high energies. Although the two GX 339-4 observations are quite close in time, there are significant differences between them. In particular, the shape of the QPO peak is quite different. Another noticeable feature is the comparatively broad shape of the band-limited noise component, which deviates from a simple Lorentzian shape. In view of the limited quality of the power spectra, we did not include QPO harmonics higher than the first. Moreover, no shoulder component was used: although the shape of the QPO peak is evidently asymmetric, it is clear from its shape that the addition of a Lorentzian shoulder would not be a reasonable approximation to its shape. The energy dependence of relevant parameters is shown in Fig. 5.

4.4. Variations in the QPO frequency

As we have seen, the central frequency of the QPO does not vary with energy. The complicated shape of the QPO peaks, with their high-frequency shoulder and differences between observations, suggests that there might be changes in the QPO central frequencies within a single observation, which would then lead to a distorted and broadened average peak in the power spectrum. To test this, we produced power spectra for different parts of the Jan 11 observation of GS 1124-68. The first part of the observation ($\sim$37 minutes) show a corrected MPC3 count-rate of 2315 cts/s in the 9.3-37.2 keV band (where the flux is dominated by the hard spectral component), while in the rest of the observation the average count-rate in the same band is 2222 cts/s. We produced separate power spectra from these two parts of the observation and then compared the QPO peaks in the lowest and highest energy bands. As it can be seen in Fig. 6, the QPO central frequency from the high-rate data is lower than the one from low-rate data by $\sim$0.2 Hz. The shapes of the two peaks are consistent with being the same. Notice that, within this observation, the QPO frequency therefore *increases* with the count rate, opposite to the variations found between different observations by Takizawa et al. (1996).

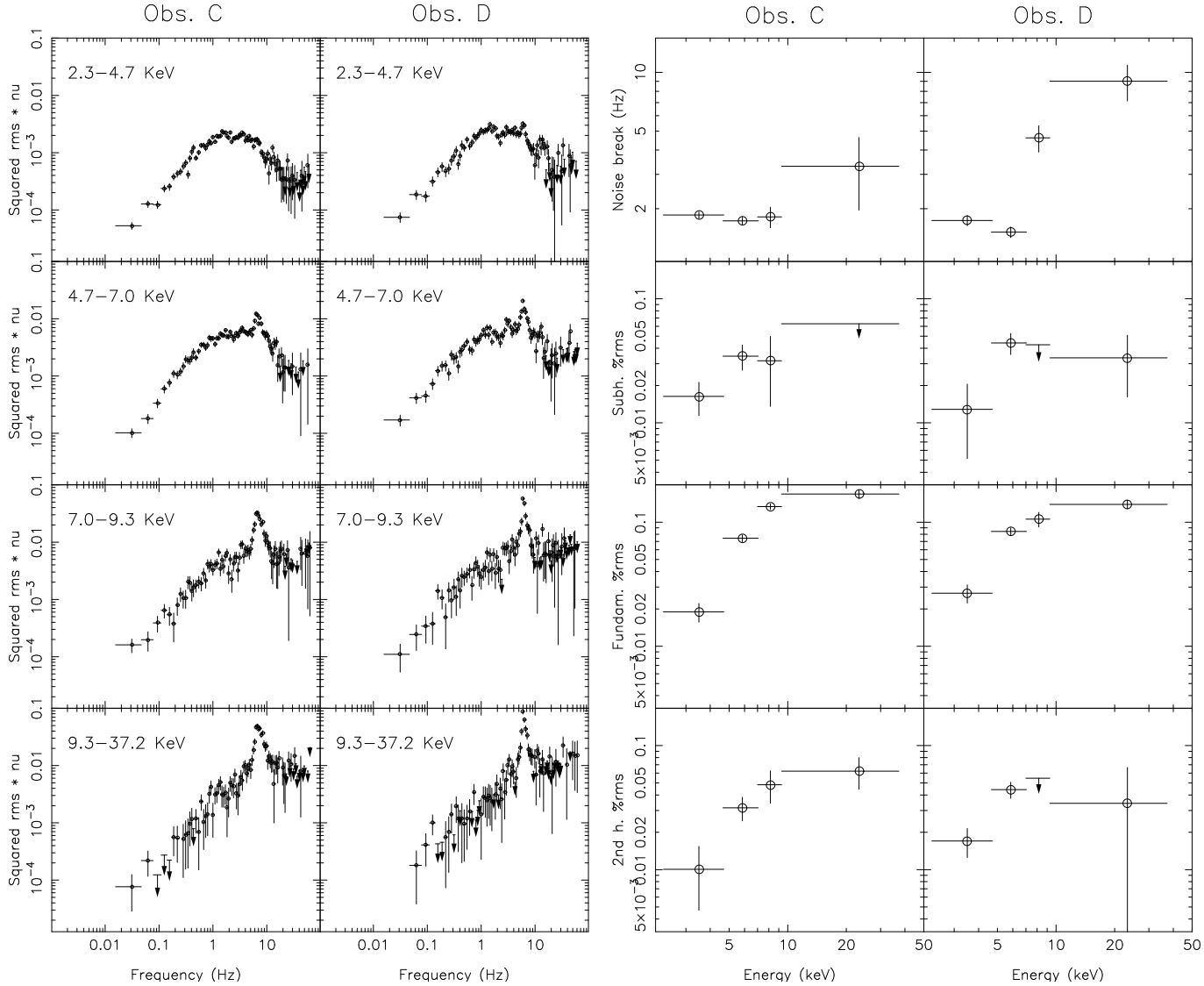

Fig. 5. Left panel: Power spectra of GX 339-4 for the two observations described in the text. The different energy bands are indicated in the labels. The power spectra are plotted following the representation described in Sect. 3. Right panel: Energy dependence of selected fit parameters.

5. Discussion

A quantitative analysis of the variation of rms strength of the different components as a function of energy is complicated by the presence of the soft spectral component, which has been reported not to contribute to either the band-limited noise or the QPO (Miyamoto et al. 1994b). A detailed spectral analysis would be necessary, but is not possible due to the lack of spectral resolution in the MPC3 data and by the relatively complicated source spectrum. The main results we describe here are independent of absolute levels in the power spectra.

5.1. The band-limited noise

The strong energy dependence of the cut-off frequency of the band-limited noise observed in both sources establishes a strong connection between the timing and spectral features of the emission. This is equivalent to a strong time dependence of the spectral distribution on sub-second timescales. Let us take the Jan 11 observation of GS 1124-68 where this effect is observed best. Notice that in many power spectra the shape of the band-limited noise appears to be broader than a simple Lorentzian, which is the main reason for the low quality of the fits. The Lorentzian fit to the power spectra, excluding for the moment the QPO, can be interpreted in terms of a simple shot noise model, i.e., a superposition of randomly occurring shots of sharp rise and exponential decay (or vice versa), all with the same shape. Since hard lags have been observed both for GS 1124-68 and GX 339-4 (see Miyamoto et al. 1991; Miyamoto et al. 1993), we adopt exponentially rising shots. Both the amplitude and the rise timescale of the shots could show an energy dependence (see Van der Klis 1988, Miyamoto & Kitamoto 1989), so

$$s(t;E) = N(E) \cdot e^{t/\tau(E)} \quad (7)$$

Table 3. Best-fit values for the parameters not included in Table 2. Errors are 1σ, upper limits are 2σ.

Energy (keV)	R_{BLN} (%)	ν_{QPO}	Δ_{QPO}	ν_{SHL}	Δ_{SHL}	f	χ^2
			GS 1124–68 – 1991 Jan 11				
3.50 ±1.20	$(7.12^{+0.10}_{-0.11})$	$5.29^{+0.02}_{-0.03}$	$0.72^{+0.08}_{-0.07}$	$5.99^{+0.17}_{-0.17}$	$1.30^{+0.21}_{-0.22}$	$0.61^{+1.21}_{-0.34}$	195.0 (121)
5.85 ±1.15	$(12.2^{+0.80}_{-0.30})$	$5.31^{+0.01}_{-0.01}$	$0.68^{+0.05}_{-0.05}$	$6.09^{+0.22}_{-0.12}$	$2.53^{+0.11}_{-0.32}$	$0.87^{+0.40}_{-0.36}$	182.0 (125)
8.15 ±1.15	$(14.5^{+1.20}_{-1.50})$	$5.28^{+0.01}_{-0.02}$	$0.54^{+0.04}_{-0.04}$	$6.20^{+0.18}_{-0.15}$	$1.79^{+0.18}_{-0.13}$	$0.47^{+0.11}_{-0.13}$	147.0 (122)
23.25±13.95	$(17.0^{+0.70}_{-0.70})$	$5.30^{+0.01}_{-0.02}$	$0.60^{+0.03}_{-0.06}$	$6.17^{+0.15}_{-0.12}$	$1.96^{+0.20}_{-0.17}$	$0.70^{+0.17}_{-0.16}$	163.0 (126)
			GS 1124–68 – 1991 Jan 22				
3.50 ±1.20	$(13.5^{+0.30}_{-0.40})$	8.21 (FIX)	2.70 (FIX)	13.50 (FIX)	3.00 (FIX)	0.25 (FIX)	109.0 (91)
5.85 ±1.15	$(10.5^{+0.30}_{-0.60})$	$8.21^{+0.08}_{-0.09}$	$2.70^{+0.29}_{-0.28}$	13.50 (FIX)	3.00 (FIX)	0.25 (FIX)	150.0 (130)
8.15 ±1.15	$(9.13^{+1.26}_{-0.70})$	$8.29^{+0.05}_{-0.04}$	$2.95^{+0.12}_{-0.17}$	$13.49^{+0.45}_{-0.45}$	$3.49^{+9.03}_{-0.69}$	$0.30^{+1.47}_{-0.04}$	130.0 (127)
23.25±13.95	$(15.8^{+1.20}_{-0.90})$	$8.39^{+0.03}_{-0.03}$	$2.66^{+0.08}_{-0.10}$	$13.95^{+0.47}_{-0.45}$	$3.06^{+1.30}_{-0.91}$	$0.23^{+0.09}_{-0.07}$	125.0 (128)
			GS 1124–68 – 1991 Jan 25				
3.50 ±1.20	$(1.18^{+0.19}_{-0.19})$	5.80 (FIX)	0.60 (FIX)	—	—	—	138.0 (135)
5.85 ±1.15	$(2.45^{+0.62}_{-0.62})$	$5.88^{+0.04}_{-0.04}$	$0.62^{+0.07}_{-0.06}$	—	—	—	155.0 (133)
8.15 ±1.15	$(3.41^{+3.02}_{-2.56})$	$5.82^{+0.03}_{-0.03}$	$0.55^{+0.08}_{-0.08}$	—	—	—	119.0 (133)
23.25±13.95	< 9.32	$5.87^{+0.03}_{-0.03}$	$0.62^{+0.08}_{-0.07}$	—	—	—	112.0 (134)
			GS 1124–68 – 1991 May 17				
3.50 ±1.20	$(7.23^{+0.49}_{-0.49})$	6.67 (FIX)	0.99 (FIX)	—	—	—	122.0 (107)
22.1 ± 15.1	$(22.4^{+2.30}_{-2.80})$	$6.67^{+0.15}_{-0.14}$	$0.99^{+0.51}_{-0.54}$	—	—	—	113.0 (104)
			GX 339–4 – Observ. C				
3.50 ±1.20	$(10.9^{+0.30}_{-0.30})$	6.70 (FIX)	2.80 (FIX)	—	—	—	137.0 (86)
5.85 ±1.15	$(17.2^{+0.60}_{-0.60})$	$6.71^{+0.07}_{-0.07}$	$2.82^{+0.21}_{-0.21}$	—	—	—	121.0 (85)
8.15 ±1.15	$(15.3^{+1.40}_{-1.30})$	$6.84^{+0.06}_{-0.06}$	$2.61^{+0.20}_{-0.18}$	—	—	—	103.0 (88)
23.25±13.95	$(13.8^{+4.40}_{-2.90})$	$7.04^{+0.07}_{-0.07}$	$2.84^{+0.23}_{-0.22}$	—	—	—	101.0 (89)
			GX 339–4 – Observ. D				
3.50 ±1.20	$(12.0^{+0.50}_{-0.40})$	$6.07^{+0.08}_{-0.08}$	$1.52^{+0.29}_{-0.28}$	—	—	—	135.0 (88)
5.85 ±1.15	$(17.3^{+0.70}_{-0.90})$	$6.10^{+0.05}_{-0.05}$	$1.82^{+0.15}_{-0.13}$	—	—	—	115.0 (88)
8.15 ±1.15	$(21.5^{+2.30}_{-2.80})$	$6.14^{+0.04}_{-0.03}$	$0.84^{+0.17}_{-0.13}$	—	—	—	114.0 (90)
23.25±13.95	$(20.0^{+3.90}_{-4.30})$	$6.12^{+0.04}_{-0.04}$	$1.02^{+0.13}_{-0.13}$	—	—	—	85.5 (88)

The observed energy spectrum over a timescale long compared to τ will come from the superposition of a number of shots and will therefore, apart from the constant, be given by the integral of one shot

$$S(E) = \int_0^\infty s(t;E)dt \tag{8}$$

For simplicity we consider the case in which the X-ray flux consists entirely of shots, without an additional DC level, so that the additional constant is zero. From Fig. 4 we can see that for Jan 11 the break frequency (the inverse of the τ parameter is a linear function of energy, from which:

$$\tau(E) \sim E^{-1} \tag{9}$$

and therefore

$$S(E) = N(E) \cdot E^{-1} \tag{10}$$

Since the observed energy spectrum for the component responsible for the variability is a power law with photon index $\Gamma \sim$2.6 (Ebisawa et al. 1994), this implies that the energy spectrum at the beginning of a shot will start with a soft energy spectrum and quickly harden with time until its peak, when the slope is 1.6.

Although the adopted model is rather simplified, it exemplifies how the energy dependence of the noise parameters translates into fast time variations of the spectral distribution. Most of the models for the interpretation of spectra from black hole candidates have ignored the fast time variability, focussing of the interpretation of average spectra (see e.g. Chakrabarti & Titarchuk 1995). The present results show that timing effects cannot be ignored. It should be noticed that a crucial parameter which drives the effect that ou results has on time-averaged energy spectra is the percentage of DC level in the flux. This effect is largest in absence of non-variable X-ray flux.

It is interesting to note that this model predicts phase lags qualitatively similar to the ones observed in both sources (see Miyamoto et al. 1993), although a more detailed analysis is needed. Since hard lags are observed, these results point to exponential-rise/sharp decay for the shot shape.

5.2. The QPO

As is apparent from the different panels of Fig. 3, the central frequency of the QPO peak is different between the GS 1124-68 observations. The results of the analysis of these variations are reported in Takizawa et al. (1996), with the exception of the May 17 QPO. We do not detect any significant dependence of the QPO frequency on energy.

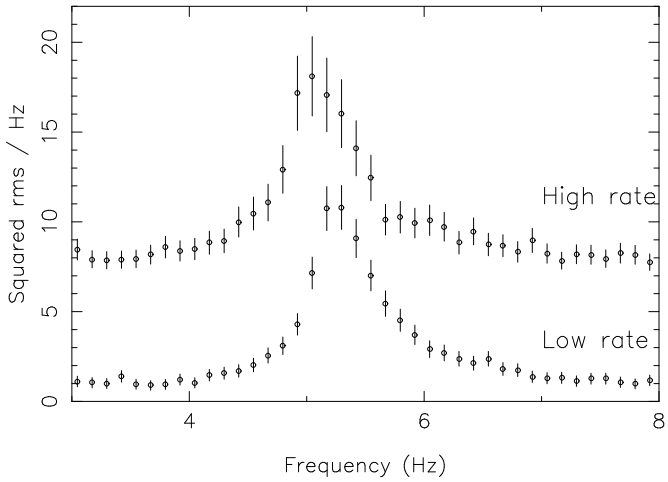

Fig. 6. QPO peaks in the power spectra of the high-rate and low-rate parts of the Jan 11 observation of GS 1126-68. The data are from the high energy band (9.3-37.2 keV). The high-rate spectrum is shifted upwards for clarity.

In all the observations of both sources, the rms of the QPO peak is higher at higher energies (see Figs. 3 and 4). However, the rms is calculated by using the total count-rate of the source in the given energy band. Since the energy spectrum consists of two components whose relative strength is different in different energy bands, this simple comparison might be misleading. If we assume that both QPO and band-limited noise occur in the same spectral component, we can compare the percentage rms in the QPO peaks with the level of the band-limited noise at low frequency, which does not show large variations with energy. We conclude that, under this assumption, the strength of the fundamental peak of the QPO indeed increases with energy, independent of the presence of two spectral components.

Another important question to be answered is whether the harmonic content of the QPO also varies with energy. For all the observations where more than one QPO peak is visible, the rms of the fundamental varies over almost an order of magnitude with energy, while all the other harmonic components do not show such extreme variations. This is particularly evident by looking at the Jan 11 power spectra in Fig. 3. We can conclude that the QPO harmonic content *decreases* with energy, which in time domain means that the higher the energy band the more "sinusoidal" the QPO cycle becomes.

In the adopted fit function, the harmonics of the QPO within one observation have harmonically related widths, as suggested by the Jan 11 observation of GS 1124-68. This has an important implication for the nature of the quasi-periodicity. The two simplest models for the production of a broad peak in a power spectrum are amplitude modulation and frequency modulation of a coherent signal. In case the underlying signal is purely sinusoidal, it is not possible to distinguish between the two cases. However, in the presence of harmonics, the two cases give different power spectra. In the amplitude modulation scenario, the width of the peaks is related to the shape of the modulation function (a window function), and therefore the absolute width of all the peaks will be the same. However, if the frequency rather than the amplitude is modulated in time, the relative modulation of the harmonics is the same, and so the *relative* width of the peaks will be the same (see Van der Klis 1991). Thus, the observation of peaks like those observed in the first column of Fig. 3 is a clear indication that the large width of the QPO is due mostly to frequency modulation or, in other words, that the presence of amplitude modulations must be limited to a window function whose broadening of QPO peaks is not larger than the width of the lowest observed harmonics. Notice that the alternative model of constant width for all the QPO peaks can be rejected with high confidence in the fits. It is interesting to notice that in the only case so far where a QPO could be observed directly in the time domain (for the Rapid Burster), the quasi-periodic nature of the oscillation was established to be due to frequency modulation (Dotani et al. 1990).

The detection of a QPO peak in the May 17 observation of GS 1124-68 deserves additional attention. It has been assumed that the VHS and the appearance of a high-frequency QPO are associated to an accretion rate close to the Eddington limit (see Van der Klis 1995). In transient sources, as the accretion rate decreases with time, the source moves to the HS and then, at low rates, to the LS. The May 17 observation is located in time between the HS and the LS: its timing properties however are similar to those of the VHS, including the presence of an energy dependent QPO peak centered at $\sim$6.7 Hz reported in the present paper. The power law photon index of the hard component during that observation is $\Gamma \sim 2.2$, intermediate between the values for VHS ($\sim$2.6) and LS ($\sim$1.6) (Ebisawa et al. 1994). The observation took place several months after the peak of the outburst, and the source flux was lower by a factor of $\sim$10 than at peak (see Ebisawa et al. 1994); it is likely that the accretion rate then was lower than the Eddington limit. Notice that variations observed in the QPO central frequency within the Jan 11 observation of GS 1124-68 do not fit either of the two frequency-intensity relations reported in Takizawa et al. (1996). It is therefore possible to have a VHS even at much lower luminosities than it has been assumed so far. In this respect it is interesting to notice that a similar power spectrum, although with a much poorer statistics which would not have allowed the detection of a QPO, was also observed with EXOSAT from GX 339-4 (Belloni and Hasinger 1990a).

The asymmetry of the shape of the QPO peaks could be interpreted as time variations of the QPO central frequency. However, this interpretation is unlikely; from the analysis of the Jan 11 observation of GS 1124-68 (see section 4.4): the QPO central frequency is observed to vary, but the (asymmetric) shape of the peak is constant within the errors. Any variation responsible for the asymmetry should therefore happen on a relatively short timescale. Alternatively, the intrinsic shape of the QPO is asymmetric and therefore not Lorentzian.

The presence of power at half the QPO period (the subharmonic) is difficult to interpret. Its relative low rms compared to the fundamental indicates that the variations of the amplitude of the quasi-periodicity which are associated with it are rather

small. In absence of a physical model for the quasi-periodicity it is premature to speculate about its origin. As mentioned in Sect. 4.1, an alternative interpretation of the multiple peaks is possible by considering what we called subharmonic to be the fundamental. In this case only even harmonics would be visible, and the fundamental would be very weak at low energy. Moreover, the oscillation would be dominated by the first harmonic.

The adopted model fixes an harmonic relation between the QPO peaks. Although from simple lorentzian fits this appears to be the case, it cannot be excluded that with a more complex model their frequencies would result not to be harmonically related.

6. Conclusions

We produced energy-resolved power spectra from Ginga observations of GS 1124-68 and GX 339-4 in the Very High State. We can summarize our results in the following way:

- The band-limited noise has a characteristic frequency that strongly increases with energy.
- The main QPO peak and its harmonics are not symmetric, but show an excess on the high-frequency wing. The fractional variability of the QPO increases with energy, while the harmonic content decreases. A considerable number of harmonic peaks is detected, whose relative width is consistent with being the same.
- An energy dependent QPO peak at $\sim$6.7 Hz has been discovered in the power spectrum of GS 1124-68 four months after the peak of the outburst
- The central frequency of the QPO of GS 1124-68 showed changes anticorrelated with the high-energy count-rates within a single observation early in the outburst.

These results provide a link between the spectral and timing properties of the X-ray emission of black-hole candidates. The detection of energy variations in the characteristic frequency of the band-limited noise translates into fast spectral variability, on time-scales too short that it would be observable with simple spectral accumulation. As a consequence, the observed energy spectrum is the integral over time of a time-variable spectrum and does not reflect the actual instantaneous spectral distribution at the source. A more detailed model of the band-limited noise is needed in order to extract quantitative information from the data, as its shape deviates from a Lorentzian, making the quality of the fits in many cases not formally acceptable. The same can be said of the QPO peaks, whose shape is clearly asymmetric and requires an excess at high frequencies.

Acknowledgements.
TB is supported by EEC under grant ERB4001GT932057. WHGL acknowledges support from the US National Aeronautics and Space Administration.

References

Belloni, T., & Hasinger, G., 1990a, A&A, 227, L33.
Belloni, T., & Hasinger, G., 1990b, A&A, 230, 103.
Chakrabarti, S.K., & Titarchuk, L.G., 1995, ApJ, 455, 623.
Dotani, T., Mitsuda, K., Inoue, H., et al., ApJ, 350, 395.
Ebisawa, K., Ogawa, M., Aoki, T., et al., 1994, PASJ, 46, 375.
Miyamoto S., & Kitamoto S., 1989, Nature, 342, 773.
Miyamoto S., Kimura K., Kitamoto S., Dotani T., and Ebisawa K., 1991, ApJ 383, 784
Miyamoto S., Iga, S., Kitamoto, S., & Kamado, Y., 1993 ApJ, 403, L39.
Miyamoto, S., Kitamoto, S., Iga, S., Hayashida, K., & Terada, K., 1994a, ApJ, 435, 398.
Miyamoto, S., Kitamoto, S., Kamado, Y., et al., 1994b, in "New Horizon of X-ray Astronomy", eds. Makino, F. & Ohashi, T., Universal Academy Press, Tokyo, p47.
Takizawa, M., Dotani, T., Mitsuda, K., Matsuba, E., Ogawa, M., Aoki, T., Asai, K., Ebisawa, K., Makishima, K., Miyamoto, S., Iga, S., Vaughan, B., Rutledge, R.E. & Lewin, W.H.G., 1996, in preparation.
Tananbaum, H., Gursky, H., Kellogg., E., Giacconi, R., & Jones, C., 1972, ApJ, 177, L5.
Turner, M.J.L, Thomas, H.W, Patchett, B.E., et al., 1989, PASJ, 41, 345.
Van der Klis, M., 1988, Adv. Space Res., 8, 383.
Van der Klis, M., 1991, in "Neutron Stars: Theory and Observations", eds. Ventura, J., and Pines, D., NATO ASI Series n.344, Kluwer Academic Publishers, p. 319.
Van der Klis, M., 1995, in "X-ray binaries", eds. Lewin, W.H.G., Van Paradijs, J., and Van den Heuvel, E.P.J., Cambridge University Press, Cambridge, p. 252.

This article was processed by the author using Springer-Verlag LaTeX A&A style file *L-AA* version 3.